

Ordering and Demixing Transitions in Multicomponent Widom–Rowlinson Models

J.L. Lebowitz

Dept. of Mathematics and Physics, Rutgers University, New Brunswick, N.J. 08903, USA

A. Mazel

Dept. of Mathematics, Rutgers University, New Brunswick, N.J. 08903, USA

*International Institute of Earthquake Prediction Theory and Mathematical Geophysics, Moscow
113556, Russia*

P. Nielaba

Institut für Physik, Johannes–Gutenberg–Universität, D–55099 Mainz, Germany

L. Šamaj*

Courant Institute, New York University, 251 Mercer Street, New York, N.Y. 10012–1185, USA

(June 13, 2021)

Abstract

We use Monte Carlo techniques and analytical methods to study the phase diagram of multicomponent Widom–Rowlinson models on a square lattice: there are M species all with the same fugacity z and a nearest neighbor hard core exclusion between unlike particles. Simulations show that for M between two and six there is a direct transition from the gas phase at $z < z_d(M)$ to a demixed phase consisting mostly of one species at $z > z_d(M)$ while for $M \geq 7$ there is an intermediate “crystal phase” for z lying between $z_c(M)$ and $z_d(M)$. In this phase, which is driven by entropy, particles, independent of species, preferentially occupy one of the sublattices, i.e. spatial symmetry

but not particle symmetry is broken. The transition at $z_d(M)$ appears to be first order for $M \geq 5$ putting it in the Potts model universality class. For large M the transition between the crystalline and demixed phase at $z_d(M)$ can be proven to be first order with $z_d(M) \sim M - 2 + 1/M + \dots$, while $z_c(M)$ is argued to behave as λ_{cr}/M , with λ_{cr} the value of the fugacity at which the one component hard square lattice gas has a transition, and to be always of the Ising type. Explicit calculations for the Bethe lattice with the coordination number $q = 4$ give results similar to those for the square lattice except that the transition at $z_d(M)$ becomes first order at $M > 2$. This happens for all q , consistent with the model being in the Potts universality class.

PACS numbers: 64.60.Cn, 05.50.+q, 02.70.Lq, 75.10.Hk

I. INTRODUCTION

In 1970 Widom and Rowlinson (WR) introduced an ingeniously simple model for the study of phase transitions in continuum fluids [1]. It consists of two species of particles, A and B, in which the only interaction is a hard core exclusion between particles of unlike species, i.e. the pair potential $v_{\alpha\beta}(r)$ is infinite if $\alpha \neq \beta$, and $r < R_{AB}$, and is zero otherwise. WR showed how this model can be transformed (by integrating over the coordinates of one species) into a one component model with explicit many body interactions. The A-B symmetry of the demixing phase transition in the original model, assumed by WR to occur in dimensions $\nu \geq 2$ when the fugacity, $z_A = z_B = z$ is large, then yields interesting information about the corresponding liquid-vapor transition in the transformed model [1].

A rigorous proof of the existence of a demixing transition in this model was given by Ruelle [2]. Ruelle used a brilliant adaptation of the Peierls argument for the Ising model on a lattice which exploits the A-B symmetry. Further results were obtained in [3]. Ruelle's proof, which permits also a smaller hard core $R_{AA} = R_{BB} < (\sqrt{3}/2)R_{AB}$ between like particles, was generalized by Lebowitz and Lieb [4] to the case where $v_{AB}(r)$ is large positive but not infinite. An extension of the proof to non-symmetric multicomponent models was made by Bricmont, Kuroda and Lebowitz using Pirogov-Sinai theory [5]. We refer the reader to [5] and references there for additional results on these WR models which are, as far as we know, the only continuum systems with fixed decaying potentials where one has been able to prove rigorously the existence of phase transitions.

The lattice version of the multicomponent WR model—hard core exclusion between particles of M different species on nearest neighbor sites of a simple cubic lattice in ν -dimensions—is much easier to handle rigorously. A proof of the demixing transition and much more, e.g. existence of sharp interfaces between coexisting phases, in $\nu \geq 3$, at large fugacity $z > z_d(M)$, can be obtained using standard Peierls methods, see [6], [7]. A rather surprising result (at least on first sight) was found by Runnels and Lebowitz [8]. They proved that when the number of components M is larger than some minimum M_0 then the

transition from the gas phase at small values of z to the demixed phase at large values of z does not take place directly. Instead there is, at intermediate values of z , $z_c < z < z_d$, an ordered phase in which one of the sublattices (even or odd) is preferentially occupied, i.e. there is a crystalline (antiferromagnetically ordered) phase in which the average particle density on the even and odd sublattices, ρ_e and ρ_o are unequal. The average density of species $I = 1, \dots, M$, $\rho(I)$, is the same on each sublattice and equal $\rho_e(I) = M^{-1}\rho_e$ and $\rho_o(I) = M^{-1}\rho_o$. The nature of the symmetry breaking is thus very different from that in the demixed phase at $z > z_d$ where $\rho_e = \rho_o = \rho$ but there exists one species, say I' , for which $\rho(I') > M^{-1}\rho$. The origin of the spatial symmetry breaking leading to the crystal phase is purely entropic. For z fixed, and M going to infinity it pays for the system entropywise to occupy just one sublattice without any constraint; there being no interaction between particles on the same sublattice each site can be occupied independently by a particle of any species, i.e. if we keep one of the sublattices empty then there are M independent choices at each site of the other sublattice. This more than compensates, at $M > M_0$, for the “loss” of fugacity occasioned by keeping down the density in the other sublattice. Put in another way, for M large enough, the typical occupancy pattern on a lattice (ignoring the label I of the particles) should behave like a one component lattice gas with nearest neighbor hard core exclusion for which Dobrushin [9] proved the existence of a crystalline state.

Once this is understood the natural question is, just how big does M_0 have to be to see this ordered phase for $M \geq M_0$. It was shown in [8] that $M_0 < 27^6$; a ridiculously large upper bound. On the other hand application of Pirogov-Sinai theory as in [10] where a similar model, in which there is a positive energy $U < \infty$ when neighboring sites are occupied by different species, is considered can probably be made to give $M_0 \lesssim 25$ for our model corresponding to $U = \infty$. Furthermore, a direct computation on the Bethe lattice with q -neighbors, gives $M_0 = [q/(q-2)]^2$, which would suggest $M_0 \sim 4$ for the square lattice. The Monte Carlo (MC) simulations presented here grew out from a desire to answer this question and to get a general picture of the phase diagram of this system in the $M - z$ plane. This we succeeded in doing, with the large M analytic results smoothly matching up

with the MC small M results and with the “dilute lattice model” investigated in [10]. The outline of the rest of the paper is as follows. In Section II we investigate the large M behavior of the model, Bethe lattice computations are given in Section III and MC simulations in Section IV.

II. ASYMPTOTICS OF THE PHASE DIAGRAM

We consider a two dimensional square lattice \mathbf{Z}^2 . Each lattice site can be either empty ($I = 0$) or singly occupied by a particle of type $I = 1, 2, \dots, M$. All the components have the same activity z and there is an infinite repulsive interaction between particles of different type on nearest neighbor sites. Thus a particle of type I at lattice site i can only have vacancies or particles of type I on nearest neighbor lattice sites. The interaction potential $\phi_{I,J}(i, j)$ between a particle of type I at site i and a particle of type J at site j is:

$$\phi_{I,J}(i, j) = \begin{cases} \infty & \text{if } i \text{ and } j \text{ are nearest neighbors and } I \neq J, I \neq 0, J \neq 0 \\ 0 & \text{otherwise} \end{cases} \quad (1)$$

It is clear that if we replace ∞ in (1) by some $U \neq 0$ then our system is equivalent to a dilute Potts model. In such a system some lattice sites are empty while others are occupied, with a weight given by the fugacity z , by an M -component Potts variable with nearest neighbor interaction between like states equal to $-U$. The WR system (1) can thus be considered as the zero temperature limit of such a model with $U > 0$. We refer the reader to [10] for a general discussion of the phase diagram of such models.

A. The Boundary Between Disordered and Crystal Phases

We will argue here that the asymptotics, as $M \rightarrow \infty$, of the boundary $z = z_c(M)$ between disordered and crystal phases is given by the hyperbola $Mz = \lambda_{cr}$, where λ_{cr} is the critical fugacity of the one-component lattice gas with the nearest-neighbor hard-core exclusion.

In the latter model every site of the lattice can be occupied by a particle with fugacity $\lambda > 0$. Hard-core repulsion requires that occupied sites are not nearest neighbors. It is well

known [11] that for this model there exists a critical fugacity $\lambda_{cr} \sim 3.7962$ such that for $\lambda < \lambda_{cr}$ the model possesses a unique limit Gibbs state (disordered phase) while for $\lambda > \lambda_{cr}$ it has at least two different limit Gibbs state (crystal phases). In one of the crystal phases the probability of the even site to be occupied by a particle is greater than that of the odd site and vice versa for the other crystal phase.

Consider now a model with M different species in which we forbid particles of any type to be nearest neighbors. Then, for fixed $\lambda = Mz$, this system is equivalent to the one-component lattice gas just described. Hence the multi-component WR system, where particles of the same type can occupy neighboring lattice sites is, in a sense, the one-component system with the hard-core condition being slightly relaxed. That naturally leads to a conjecture that for $Mz \leq \lambda_{cr}$ our multicomponent system is in the disordered phase.

Speaking more precisely, any configuration of the multicomponent system (1) can be uniquely decomposed on the connected components of the occupied sites. The connected component consisting of a single site can be interpreted as a hard-core particle with the fugacity Mz as we do not specify the type of the particle. Other connected components consisting of $n \geq 2$ sites we call clusters. All the particles in the cluster are of the same type and the fugacity of the cluster is Mz^n , as we again do not specify the type of the particles in the cluster. Note that this representation naturally extends the multicomponent model to non integer values of M .

It is obvious that the fugacity of clusters tends to 0 as $z \rightarrow 0$, $\lambda = Mz$ fixed, and the free energy of the multicomponent model tends to the free energy of the one-component hard-core gas with the fugacity λ , i.e. the contribution of the clusters becomes negligible in the limit $z \rightarrow 0$, with $\lambda = Mz$ fixed. This suggests that in the (M, z) plane there exists a curve $M = M_c(z)$, with $M_c(z) \rightarrow \lambda_{cr}/z$ as $z \rightarrow 0$, on which there is the second order phase transition between disordered and crystal phases. The typical configuration of the crystal phase has one sublattice, say the even one, occupied by particles except for rare excitation "islands", where every "island" is either a cluster or has the structure of the opposite crystal phase with occupied odd sublattice.

B. The Boundary Between Crystal and Demixed Phases

The boundary between crystal and demixed phases admits a rigorous analysis in the framework of the Pirogov-Sinai theory (see [12], [13], [14]). Related general results for the wider class of models including our multi-component system can be found in [10]. Here we present a more detailed analysis by means of a direct "elementary" approach.

Given a configuration of the multi-component system we say that this configuration at a site of the lattice \mathbf{Z}^2 is,

(i) in the demixed phase I , if this site and at least one of its nearest neighbor sites are occupied by particles of type I ;

(ii) in the odd crystal phase, if this site is even and empty or is odd and occupied by a particle (of any type) while all four nearest neighbor sites are empty;

(iii) in the even crystal phase, if this site is odd and empty or is even and occupied by a particle (of any type) while all four nearest neighbor sites are empty.

It is not hard to check that the statistical weight of an arbitrary configuration can be calculated as the product over all unit bonds of the lattice \mathbf{Z}^2 of the following statistical weights of the bonds:

(i) $z^{1/2}$ for the bond joining two sites in the same demixed phase;

(ii) $(Mz)^{1/4}$ for the bond joining two sites in the same crystal phase (necessarily one of the sites is occupied and other is empty);

(iii) 1 for the bond joining sites in the different crystal phases (necessarily both sites are empty);

(iv) $z^{1/4}$ for the bond joining sites in the crystal and demixed phases (the site in the crystal phase is necessarily empty).

All other bonds are forbidden, i.e. they have a zero statistical weight. Without changing the Gibbs distribution we multiply all statistical weights of the bonds by $z^{-1/2}$ and obtain renormalized statistical weights 1, $(M/z)^{1/4}$, $z^{-1/2}$ and $z^{-1/4}$ respectively. From that picture it is clear that for $1 \leq M < z$ the configurations with all sites being in the same demixed

phase are the only periodic ground states (i.e. the configurations minimizing the specific energy) of the model (there are M of them). For $0 < z < M$ the configurations with all sites being in the same crystal phase are the only periodic ground states of the model (there are 2 of them). Finally on the line $M = z$ all $M + 2$ configurations above are the ground states of the model and there is no other periodic ground state.

Given a configuration we introduce the Peierls contours as the connected components of the unit bonds of the dual lattice $\tilde{\mathbf{Z}}^2 = \mathbf{Z}^2 + (1/2, 1/2)$ separating sites of \mathbf{Z}^2 not in the same phase. It is not hard to see that every configuration has an equivalent representation in terms of a collection of mutually disjoint Peierls contours. Moreover, on the line $M = z$ the statistical weight of the configuration is the product of the statistical weights of the contours. In turn, the statistical weight of a contour is the product of the statistical weights of the bonds of \mathbf{Z}^2 dual to the bonds of the contour. Here dual means rotated by $\pi/2$ with respect to the center of the bond. This representation is customary for the Pirogov-Sinai theory and allows complete investigation of the diagram of the periodic limit Gibbs states in the region $M \geq \max(z_0/z, 1)$ for a sufficiently large absolute constant z_0 .

Theorem. *For $M \geq \max(z_0/z, 1)$ and z_0 large enough there exists in the (M, z) plane a curve $M = M_d(z)$, $|M_d(z) - z| = O(1)$, such that on this curve all $M + 2$ ground states generate the corresponding limit Gibbs measures and these limit Gibbs measures are the only periodic limit Gibbs measures.*

For $\max(z_0/z, 1) < M < M_d(z)$ every demixed ground state generates the corresponding limit Gibbs state and these M limit Gibbs states are the only periodic limit Gibbs measures.

For $M > \max(z_0/z, 1, M_d(z))$ every crystal ground state generates the corresponding limit Gibbs state and these 2 limit Gibbs states are the only periodic limit Gibbs measures.

(See [12], [13], [14] and cf. [10]).

More precise asymptotics $M_d(z) = z + 2 - z^{-1} + O(z^{-2})$ as $z \rightarrow \infty$ can be calculated via an approach suggested in [15]. Namely, set $M_d(z) = z + \sum_{n=0}^{\infty} c_n z^{-n}$. Then one can successively calculate c_n by equating term by term the cluster or polymer expansion series

written for the specific free energies f_c and f_d of the crystal and demixed phases respectively. The definition of polymers and their statistical weights can be found in [16].

It is not hard to see that

$$f_d = -\log z - z^{-1} + \frac{1}{2}z^{-2} + O(z^{-3}),$$

where

- (i) $-\log z$ is the specific energy of the demixed ground state;
- (ii) z^{-1} is the statistical weight of the polymer consisting of a single excitation obtained from the demixed ground state by removing a particle from a given lattice site;
- (iii) $z^{-2}/2$ is the statistical weight of the polymer consisting of two copies of the excitation defined in (ii);
- (iv) $O(z^{-3})$ is the contribution of the rest of polymers.

Similarly

$$\begin{aligned} f_c &= -\frac{1}{2}\log(Mz) - \frac{1}{2}(Mz)^{-1} - \frac{1}{2}M(zM^{-4}) + O(z^{-3}) \\ &= -\log z - \frac{c_0}{2}z^{-1} - \left(\frac{c_1}{2} - \frac{c_0^2}{4} + 1\right)z^{-2} + O(z^{-3}), \end{aligned}$$

where

- (i) $-\log(Mz)/2$ is the specific energy of the crystal ground state;
- (ii) $(Mz)^{-1}$ is the statistical weight of the polymer consisting of a single excitation obtained from the crystal ground state by removing a particle from an occupied site; the factor $1/2$ is due to the fact that in the crystal ground state only one half of the lattice points are occupied;
- (iii) zM^{-4} is the statistical weight of the polymer consisting of a single excitation obtained from the crystal ground state by placing a particle of a given type I at a previously non occupied lattice site; such a particle requires the neighboring sites to be in the same phase I ; any of M types of particles can produce such an excitation which is reflected in the factor M ; finally, the factor $1/2$ is due to the fact that in the crystal ground state only one half of the lattice points is non occupied;

(iv) $O(z^{-3})$ is the contribution of the rest of polymers;

Thus equating f_d and f_c one obtains $c_0 = 2$ and $c_1 = -1$. Note that every c_n can be calculated in the same way but the amount of calculation grows very fast with n .

III. THE BETHE LATTICE COMPUTATION

We now present an exact calculation of the phase diagram for our multicomponent WR model formulated on the Bethe lattice of general coordination number q . The computation is based on the exact “inverse solution” for simply connected lattice structures [17], [18]. The approach is a more transparent alternative to the usual recursion method, it replaces the most stable fixed point criterion by the general principle of the global minimum of the free energy.

In the Bethe lattice, every vertex i is an articulation point of multiplicity q . Let us denote by $\{z_i(I), I = 0, 1, \dots, M\}$ with the reference $z_i(0) \equiv 1$ the set of fugacities assigned to the corresponding particle states at site i , and by $\{\rho_i(I)\}$ the generated particle-density field constrained by

$$\sum_{I=0}^M \rho_i(I) = 1. \quad (2)$$

A direct method assumes given fugacities $\{z_i(I)\}$ and then calculates the densities $\{\rho_i(I)\}$ and the specific free energy via the Gibbsian grand canonical ensemble formalism. In the inverse method on the contrary we calculate the specific free energy and fugacities $\{z_i(I)\}$ as functions of densities $\{\rho_i(I)\}$ considered as the basic variables. The articulation character of vertices in the Bethe lattice then permits the topological reduction of the equilibrium description. In particular:

(i) the inverse profile equation, i.e. the dependence of the fugacity field $\{z_i(I)\}$ on the specified density field $\{\rho_i(I)\}$, takes the local form [17]

$$z_i(I) = \left[\frac{\rho_i(0)}{\rho_i(I)} \right]^{q-1} \prod_{j=1}^q z_i^{<i,j>}(I). \quad (3)$$

Here and later, the superscript $\langle i, j \rangle$ refers to the model (1) on an isolated (i.e. with empty boundary conditions) bond joining two neighboring sites i and j . The partition function of this two-site model is denoted by $\Xi^{\langle i, j \rangle}$. The fugacities are denoted by $z_i^{\langle i, j \rangle}(I)$ and $z_j^{\langle i, j \rangle}(I)$. The densities are $\{\rho_i(I)\}$ and $\{\rho_j(I)\}$. In the notation for densities the superscript is omitted as these densities coincide with actual ones on the Bethe lattice which we always assume to be *specified*.

(ii) The Helmholtz free energy of a system expressed via densities, $F[\rho] = -\log \Xi + \sum_{i,I} \rho_i(I) \log z_i(I)$ with Ξ being the grand partition function, can be calculated as (see [18])

$$F[\rho] = \sum_{\langle i, j \rangle} F^{\langle i, j \rangle}[\rho_i, \rho_j] - (q-1) \sum_i F^i[\rho_i], \quad (4)$$

where the summation over $\langle i, j \rangle$ is over every pair of nearest neighbors. The one-site and the two-site Helmholtz free energies are

$$F^i[\rho_i] = -\log \Xi^i + \sum_{I=0}^M \rho_i(I) \log z_i(I) = \sum_{I=0}^M \rho_i(I) \log \rho_i(I) \quad (5)$$

and

$$F^{\langle i, j \rangle}[\rho_i, \rho_j] = -\log \Xi^{\langle i, j \rangle} + \sum_{I=0}^M \rho_i(I) \log z_i(I) + \sum_{I=0}^M \rho_j(I) \log z_j(I). \quad (6)$$

In order to mimic realistically a non-simply connected structure of the same coordination q , it is necessary to avoid the effect of the large number of boundary sites of the Cayley tree. This can be done by assuming that, in the thermodynamic limit, the local properties of interior vertices (expressed in terms of particle densities) are equivalent, i.e. by considering only translation-periodic extremal Gibbs measures on the Cayley tree. Under homogeneous external conditions $z_i(I) = z(I)$ for all i , the existence of a phase transition can be simply detected from (3) as a bifurcation point, resp. a ‘‘jump’’ point for the densities, with the minimum principle of the free energy, determining the right equilibrium.

A. Crystal Phase

The crystal regime of our model is characterized by the supposed symmetry-breaking in particle densities on alternating sublattices. Accordingly we set $\rho_i(I) = \rho_1$ for sites i on the

first sublattice and $\rho_j(I) = \rho_2$ for sites j on the second sublattice ($I = 1, \dots, M$). In the corresponding two-site model we suppose that $z_i^{\langle i,j \rangle}(0) = z_j^{\langle i,j \rangle}(0) = 1$, $z_i^{\langle i,j \rangle}(I) = z_1$ and $z_j^{\langle i,j \rangle}(I) = z_2$ ($I = 1, 2, \dots, M$) since there is no preference for any component at a given sublattice. With this notation the two-site pair partition function $\Xi^{\langle i,j \rangle}$ is

$$\Xi^{\langle i,j \rangle} = 1 + M(z_1 + z_2) + Mz_1z_2 . \quad (7)$$

As functions of z_1 and z_2 the one-site particle densities ρ_1 and ρ_2 are given by

$$\rho_1 \Xi^{\langle i,j \rangle} = z_1(1 + z_2) . \quad (8a)$$

$$\rho_2 \Xi^{\langle i,j \rangle} = z_2(1 + z_1) . \quad (8b)$$

From (7), (8) we easily get $\Xi^{\langle i,j \rangle}$ and $z_{1,2}$ as functions of $\{\rho_1, \rho_2\}$:

$$z_1 = \frac{M(\rho_1 + \rho_2) - 1 + \rho_1 - \rho_2 + D^{1/2}}{2(1 - M\rho_1)} , \quad (9a)$$

$$z_2 = \frac{M(\rho_2 + \rho_1) - 1 + \rho_2 - \rho_1 + D^{1/2}}{2(1 - M\rho_2)} , \quad (9b)$$

$$\Xi^{\langle i,j \rangle} = \frac{M(M - 1)(\rho_1 + \rho_2) - (M - 2) + MD^{1/2}}{2(1 - M\rho_1)(1 - M\rho_2)} , \quad (10)$$

where the plus sign of the square root of the discriminant

$$D = [1 - (M - 1)(\rho_1 + \rho_2)]^2 + 4\rho_1\rho_2(M - 1) \quad (11)$$

is fixed by the condition $z_{1,2} \rightarrow 0$ for $\rho_{1,2} \rightarrow 0$. Finally, using (2) and (3) with homogeneous external conditions $z_i(I) = z$ for all i and $I = 1, \dots, M$, we find

$$z = \left(\frac{1 - M\rho_1}{\rho_1} \right)^{q-1} z_1^q , \quad (12a)$$

$$z = \left(\frac{1 - M\rho_2}{\rho_2} \right)^{q-1} z_2^q . \quad (12b)$$

Because of translation periodicity the free energy per site, f_c , can be determined from (4) as follows

$$f_c = -\frac{q}{2} \log \Xi^{\langle i,j \rangle} - \frac{q-1}{2} \log [(1 - M\rho_1)(1 - M\rho_2)]. \quad (13)$$

The relations (12) can be considered as the equation $z(\rho_1, \rho_2) = z(\rho_2, \rho_1)$ ($0 < \rho_1, \rho_2 < M^{-1}$). In the variables $s = (\rho_1 + \rho_2)/2$ and $t = \rho_1 - \rho_2$ it can be rewritten as $z(s, t) = z(s, -t)$ and always has a trivial solution $(s, 0)$. There is no other solution if $s \in [0, s_c^L) \cup (s_c^U, M^{-1}]$,

$$s_c^L = \frac{1}{2M}(1 - E^{1/2}), \quad (14a)$$

$$s_c^U = \frac{1}{2M}(1 + E^{1/2}), \quad (14b)$$

and

$$E = 1 - \frac{4M(q-1)}{(M-1)q^2}, \quad (15)$$

because for these s , calculated from the equation $\partial z(s, 0)/\partial t = 0$, the derivative $\partial z(s, t)/\partial t$ has a constant sign. For $s \in (s_c^L, s_c^U)$ one has a nontrivial solution to $z(s, t) = z(s, -t)$. The corresponding critical fugacities read

$$z_c^L = M^{q-1} \left(\frac{1 - E^{1/2}}{1 + E^{1/2}} \right) \left[\frac{(q-2)/q - E^{1/2}}{1 - E^{1/2}} \right]^q, \quad (16a)$$

$$z_c^U = M^{q-1} \left(\frac{1 + E^{1/2}}{1 - E^{1/2}} \right) \left[\frac{(q-2)/q + E^{1/2}}{1 + E^{1/2}} \right]^q. \quad (16b)$$

The critical point exists provided that $E \geq 0$, which imposes the requirement on the number of components $M \geq M_0$ with the minimum value M_0 given by

$$M_0 = \left(\frac{q}{q-2} \right)^2. \quad (17)$$

It is easy to verify, using (13), that the crystal phase is thermodynamically dominant (i.e. it has the minimal specific free energy) with respect to the disordered one in the interval of activities $z_c^L < z < z_c^U$. It is not hard to see that for large M

$$z_c^L \sim \frac{1}{M} \frac{(q-1)^{q-1}}{(q-2)^q} = \frac{\lambda_{cr}^{Bethe}}{M} \quad (18)$$

and

$$z_c^U \sim M^{q-1} \frac{(q-2)^q}{(q-1)^{q-1}}. \quad (19)$$

B. Demixed Phase

In the demixed phase regime, the sites are equivalent but one of components, say $I = 1$, has greater density: $\{\rho_i(1) = \rho(1), \rho_i(I) = \rho(2) \text{ for all } I = 2, \dots, M\}$. Assuming $z_i^{<i,j>}(0) = z_j^{<i,j>}(0) = 1$ and denoting $z_i^{<i,j>}(1) = z_j^{<i,j>}(1) = z(1)$, $z_i^{<i,j>}(I) = z_j^{<i,j>}(I) = z(2)$, $I = 2, \dots, M$ for the two-site model we have

$$\Xi^{<i,j>} = [1 + z(1)]^2 + (M-1)[1 + z(2)]^2 - (M-1), \quad (20)$$

$$\rho(1)\Xi^{<i,j>} = z(1)[1 + z(1)]. \quad (21a)$$

$$\rho(2)\Xi^{<i,j>} = z(2)[1 + z(2)]. \quad (21b)$$

The system of equations (3) is closed by considering $z_i(I) = z$, $I = 1, \dots, M$ and (2), which leads to the equations

$$z = \left[\frac{1 - \rho(1) - (M-1)\rho(2)}{\rho(1)} \right]^{q-1} z(1)^q. \quad (22a)$$

$$z = \left[\frac{1 - \rho(1) - (M-1)\rho(2)}{\rho(2)} \right]^{q-1} z(2)^q. \quad (22b)$$

The free energy per site is readily obtained in the form

$$f_d = -\frac{q}{2} \log \Xi^{<i,j>} - (q-1) \log[1 - \rho(1) - (M-1)\rho(2)]. \quad (23)$$

We solved the non linear equations (20)-(22) numerically. Given M , there is for small z only one solution corresponding to the disordered phase. As we increase z , two other solutions appear at some $z = \bar{z}_d(M)$. For bigger values of z even more solutions exist. It appears that among these nontrivial solutions the solution with maximal $\rho(1)$ always has the minimal free energy. We call it demixed 1 (d1) solution. Finally we calculate the phase diagram for $q = 4$ (see Fig. 1) by comparing the free energies of disordered, crystal and demixed 1 phases.

The behavior of the solutions is very similar to that of the zero-field Potts model on the Bethe lattice [19,20] (where the role of fugacity is played by the coupling constant). More precisely, simultaneously with d1 another solution, d2, appears at the point $\bar{z}_d(M)$ (see Fig. 2a). At \bar{z}_d , the free energy of d1 and d2 phases is greater than that of the disordered phase and $\rho_{d1}(1) = \rho_{d2}(1) > \rho_{dis}(1)$. Increasing z further, these two phases split and $\rho_{d1}(1) > \rho_{d2}(1)$. At $z = z_d$ (or $z = z_c$), the free energy of the d1 phase coincides with the one of the disordered (or crystal) phase, and the system exhibits a first-order phase transition, accompanied by a jump in densities $\rho_{dis}(1) \rightarrow \rho_{d1}(1)$. To complete the description, we mention that at a larger value of z , $z = \tilde{z}_d$, given by

$$\tilde{z}_d = \left(\frac{M - 2 + q}{q - 1} \right)^{q-1} \frac{1}{q - 2}, \quad (24)$$

we have $\rho_{d2}(1) = \rho_{d2}(2) = \rho_{dis}$ and the free energies of the disordered and d2 phases coincide. For $z > \tilde{z}_d$, one observes that $\rho_{d2}(1) < \rho_{d2}(2)$, i.e. one particle components is paradoxically suppressed by the others for d2 solution which has in this region a lower free energy than that of disordered phase but greater than that of d1 phase. The only exception from the above scenario is represented by the $M = 2$ component WR model (Fig. 2b). In that case, the d1 and d2 phases are in fact the equivalent realizations of the particle $1 \leftrightarrow 2$ exchange symmetry of the same demixed phase, and the corresponding demixing phase transition is of second order.

Let $M_c(\nu)$ denotes the ‘‘critical’’ number of components of the WR model in ν -dimensions, such that the phase transition from the disordered to the demixed phase is

second order for $M \leq M_c$ and first order for $M > M_c$. For the Bethe lattice, we have $M_c = 2$ independently of the coordination number. This value of M_c is exactly the same as the value of its counterpart defined for the ordinary zero-field M -state Potts model on the Bethe lattice. The equality $M_c = 2$ for the Potts model is supposed to hold for regular lattices in dimensions $\nu \geq 4$, where the mean-field treatment provides an adequate description of the critical behavior. We therefore suggest that our M -component WR model is a dilute version of the M -state Potts model, preserving the Z_M symmetry among the particle states, which falls into the same universality class. This conjecture is supported by the MC estimate $M_c = 4$ for the WR model on the $\nu = 2$ square lattice in accordance with the behavior of the Potts model on the square lattice [21]. This is discussed in the next part of the paper.

IV. MONTE CARLO SIMULATION

In this section we present results of the Monte Carlo study of the M -component WR model on a square lattice of size $S^2 = 100 \times 100$ with periodic boundary conditions. On an initially empty lattice we deposit particles chosen at random from the M components at fugacity z respecting the exclusion given by (1). We sequentially update the lattice using a checkerboard algorithm resulting in a good vectorization. An update of a lattice site (i_1, i_2) occupied by a particle of type I ($I = 0$ indicating an empty site) is done as follows: We randomly choose a new trial particle of type I_{tr} , where I_{tr} can have any integer value between 0 and M with equal probability. $I_{tr} = 0$ refers to a removal attempt of a particle $I \neq 0$ from the lattice site, which is successful, if a number X randomly chosen with equal probability between 0 and 1 is smaller than the inverse fugacity $1/z$. In this case I gets the value 0, otherwise it remains unchanged. $I_{tr} \neq 0$ refers to a deposition attempt of a particle of type I_{tr} . If $I = 0$ then it is successful if each of the four nearest neighbor sites is either empty or occupied by a particle of the same type (I_{tr}) and $X < z$. In this case I gets the value I_{tr} , otherwise it remains unchanged. A direct replacement attempt of a particle

$I \neq 0$ surrounded by four empty nearest neighbor sites is always successful. Typically in a simulation run after an equilibration of 5×10^5 Monte Carlo steps (MCS) we update the lattice 5×10^5 times (in the cases $M = 6$ and $z = 2.5, 3., 3.5$ and 4 up to 5×10^6 times), the configuration of every tenth step is taken for the evaluation of the averages. A typical run with 5×10^5 MCS took about 3 CPU hours on a CRAY-YMP.

Let $m(i_1, i_2)$ denote the occupancy of a site, $m(i_1, i_2) = 0$ if the site (i_1, i_2) is empty and $m(i_1, i_2) = 1$ otherwise. As observables we took histograms $P_L(\phi_c)$ of the order parameter ϕ_c for the crystal structure and $P_L(\phi_d)$ of the order parameter ϕ_d for the demixed phase in subsystems of size $L \times L$,

$$\phi_c = \frac{1}{L^2} \sum_{i_1, i_2=1}^L [2m(i_1, i_2) - 1] (-1)^{i_1+i_2} \quad (25)$$

and

$$\phi_d = \frac{1}{L^2} \text{Max}_I N_L(I) - \rho/M \quad (26)$$

where $N_L(I)$ denotes the number of particles of type I in a subsystem of size $L \times L$ and ρ is the average overall density.

In Fig. 3 we show typical configurations for $M = 9$ at three different values of z . In Fig. 3(a), $z = 0.1$, in this case the system is in the gas (or disordered phase). In Fig 1(b), $z = 5$, and the system is in the crystal phase where one of the sublattices has a higher density. In Fig. 3(c), $z = 8.5$ and the lattice is predominantly occupied by particles of one type (demixed regime).

We first discuss the phase transition from the gas to the crystal phase. For a given M the transition activity z_c is found by finite size scaling techniques [22,23]. In particular the k - th moments of the order parameter distribution $P_L(\phi_c)$,

$$\langle \phi_c^k \rangle_L := \int \phi_c^k P_L(\phi_c) d\phi_c \quad (27)$$

can be evaluated in subsystems of size $L \times L$, and from them the fourth order cumulant [23] U_L ,

$$U_L = 1 - \frac{\langle \phi_c^4 \rangle_L}{3 \langle \phi_c^2 \rangle_L^2}. \quad (28)$$

In a one phase region far away from a critical point the subsystem size typically can be chosen larger than the correlation length ξ , $L \gg \xi$ and the order parameter distribution is to a good approximation a Gaussian centered around 0, resulting in $U_L \rightarrow 0$ for $L \rightarrow \infty$. In the two phase coexistence region far away from a critical point we can again assume $L \gg \xi$ and the order parameter distribution is bimodal resulting in $U_L \rightarrow 2/3$ for $L \rightarrow \infty$. Near the critical point however we have $L \ll \xi$, and using scaling arguments [23] the cumulant is a function of L/ξ , resulting for $\xi \rightarrow \infty$ in the same value of U_* for all different L . This method efficiently allows the localization of critical points by analyzing the cumulants for different values of z on different length scales L . For low values of z we are in the disordered one phase region, here $U_{L'} > U_L$ for $L' < L$. For large enough M we obtain a crystal phase with $U_{L'} < U_L$ for $L' < L$. Near a critical point we should expect $U_{L'} \approx U_L$ for $L' \neq L$.

In Figs. 4-6 we present the results for U_L as a function of z . For $M = 9$ we observe in Fig. 4 a cumulant intersection near $z_c = 0.85 \pm 0.05$ indicating the phase transition from the disordered to the crystal phase. For $M = 8$ we have an intersection point at $z_c = 1.1 \pm 0.05$ (see Fig. 5) and for $M = 7$ at $z_c = 1.6 \pm 0.1$ (see Fig. 6). For $M = 20, 15, 14$ and 10 we obtain $z_c = 0.24, 0.35, 0.38, 0.68 \pm 0.01$ respectively. The transition points are presented in Fig. 7 together with the asymptotic expression [24] $Mz = 3.7962$, (section II) and the results from the Bethe lattice computation, (section III). We find good agreement of our MC results with those of the asymptotic form for large values of M and for large z with the results of the Bethe lattice computation as well.

The case $M = 6$ is analyzed in Fig. 8. In all cases studied the order parameter cumulant is decreasing with increasing system size, see Fig. 8(a), indicating the presence of the disordered phase. In Fig. 8(b) we show the cumulant for a given system size versus z , no cumulant intersection points were found in these cases, but $U_{L'} > U_L$ for $L' < L$ even for z - values as large as $z = 4.4$ indicating that the system with $M = 6$ components is in the disordered phase. Our conclusion of the data analysis is that, based upon the present statistical effort,

no sign of a phase transition from the gas phase to the crystal phase was found for $M \leq 6$, indicating the nonexistence of this transition for $M \leq 6$. Thus the minimum number of components required for the existence of the crystal phase is $M = 7$; with possibly a noninteger value M_0 between 6 and 7.

The transitions from the disordered to the crystal phase were analyzed further by finite size scaling techniques. We plotted the scaling functions of the order parameter and the order parameter susceptibility, $\tilde{\phi}_c = L^{\beta/\nu} \langle |\phi_c| \rangle_L$ and $\tilde{\chi}_c = L^{2-\gamma/\nu} [\langle \phi_c^2 \rangle_L - \langle |\phi_c| \rangle^2]$ versus the scaling variable $t = |z - z_c| L^{1/\nu}$, where β , γ and ν are the critical exponents of the order parameter, susceptibility and correlation length respectively. On a double logarithmic plot we obtained data collapses and the 2D-Ising asymptotic large- t behavior for all cases studied by utilizing the critical exponents of the 2D-Ising universality class ($\beta = 1/8$, $\gamma = 7/4$ and $\nu = 1$); examples are shown in Figs. 9, 10, 11. These data, in conjunction with the cumulant intersection value being independent of M and close to the accepted value for the 2D Ising class indicate that independent of the number of components M the transition from the disordered to the crystal phase belongs to the 2D Ising universality class.

We now discuss the phase transitions to the demixed phase. The phase transition was analyzed by a study of the order parameter distribution $P_L(\phi_d)$, the density $\rho(z)$ and free energy integration. In Fig. 12 we show the density of the system versus z for different values of M . The density is an increasing function of z and approaches for large z the asymptotic form $\rho = z/(1+z)$ which describes the behavior of the system with $M = 1$. In the demixed phase one particle type is dominant and so the system properties are close to that of a one component system. In general the density in the demixed phase exceeds the value $1/2$, for $M > 6$ we observe a direct first order transition from the crystal to the demixed phase, with a finite jump in the density at the transition fugacity z_d . For large M the density should jump from $\rho \approx 1/2$ to $\rho \approx z_d/(1+z_d)$. In the simulations we find a hysteresis region around z_d going approximately between these two values when increasing and decreasing the fugacity. In cases of a small hysteresis region with extent of less than $|z - z_d| < 0.1$ the middle z -value of this region was taken as the transition value z_d . In cases of a pronounced

hysteresis region we located the transition fugacity z_d by two independent methods. (i) We integrated the free energy from $z = 0$ to z_d and from $z = \infty$ to z_d , where the limiting free energies are known. For the low fugacity free energy we obtain:

$$p_l(z) = - \int_0^z dz_1 \rho(z_1)/z_1 \quad (29)$$

For the high fugacity free energy we obtain:

$$p_h(z) = - \int_{z_l}^z dz_1 \rho(z_1)/z_1 - \log(1 + z_l) \quad (30)$$

where z_l is chosen that large (typically $z_l = 50$) that $\rho(z_l) \approx z_l/(1 + z_l)$. The intersection value z_d , where $p_l(z_d) = p_h(z_d)$ was one estimate for the value of the fugacity where the first order transition to the demixed phase takes place, see Fig. 13. (ii) Another independent estimate for z_d was obtained by the procedure of searching for relative stability of one of the two phases during a simulation starting from configurations with both phases present in parallel slices extending over the length of the simulation box, see Fig. 13. Both independent methods gave, within 5% uncertainty, the same numerical values for z_d . The resulting phase transition values of z_d are shown in Fig. 7. We note that with increasing number of components, the transition fugacities approach the exact asymptotic line $M = z + 2 - 1/z$, see section II.

For the cases $M \geq 5$ we find a jump in the density at z_d so that we classify these transitions as first order transitions. For $M \leq 4$ we do not observe a jump in the density at z_d . In these cases the transition was located by the cumulant intersection method, see above, where the order parameter ϕ_d is the order parameter of the demixed phase and ϕ_c has to be replaced by ϕ_d in Eqs.(27) and (28). A finite size scaling analysis shows that the data for the order parameter and the susceptibility of the phase transitions for $M \leq 4$ are consistent with the 2D M -state Potts universality class, see Figs. 14, 15. For the susceptibility and $M = 4$ we obtain a much better scaling behavior compared to an analysis assuming the 2D-Ising exponents to be valid, however we note that the ratios for β/ν and γ/ν of the Potts classes [21] agree with the 2D Ising class values within a few per cents, so that a

clear distinction between these classes based on our numerical data is difficult. Recently the case $M = 2$ was studied with Monte Carlo methods [25] where evidence for the 2D-Ising universality class was found, in agreement with our findings.

ACKNOWLEDGMENTS

We thank L. Chayes and R. Kotecky for useful discussion about their work [10]. P.N. acknowledges support from the Deutsche Forschungsgemeinschaft (Heisenberg foundation), the computations were carried out at the CRAY-YMP of the RHRK Kaiserslautern. The work of J.L.L. and A.M. was supported by NSF Grant DMR 92-13424. The work of L.Š. was supported by NSF Grant CHE 92-17893.

REFERENCES

* On leave from Institute of Physics, Slovak Academy of Sciences, Bratislava, Slovak Republic

- [1] B. Widom and J.S. Rowlinson, *J. Chem. Phys.* **52**, 1670 (1970).
- [2] D. Ruelle, *Phys. Rev. Lett.* **27**, 1040 (1971).
- [3] J. Bricmont, K. Kuroda and J.L. Lebowitz, *Z. Wahrscheinlichkeitstheor. Verw. Geb.* **67**, 121 (1984).
- [4] J.L. Lebowitz and E.H. Lieb, *Phys. Lett A* **39**, 98 (1972).
- [5] J. Bricmont, J.L. Lebowitz, C.E. Pfister and E. Olivieri, *Comm. Math. Phys.*, **66**, 1 (1979)
- [6] J.L. Lebowitz and G. Gallavotti, *J. Math. Phys.* **12**, 1129 (1971).
- [7] J. Bricmont, J.L. Lebowitz, C.E. Pfister and E. Olivieri, *Comm. Math. Phys.* **66**, 127 (1979).
- [8] L.K. Runnels, J.L. Lebowitz, *J. Math. Phys.* **15**, 1712 (1974).
- [9] R.L. Dobrushin, *Funct. Anal. Appl.* **2**, 302 (1968).
- [10] L. Chayes, R. Kotecky and S.B. Shlosman, *Aggregation and Intermediate Phases in Dilute Spin Systems*, *preprint* (1994).
- [11] R.J. Baxter, I.G. Enting and S.K. Tsang, *J. Stat. Phys.* **22**, 465 (1980).
- [12] S.A. Pirogov and Ya.G. Sinai, *Phase Diagrams of the Classical Lattice Systems*, *Theor. Math. Phys.* **25**, 1185-1192 (1975) and **26** 39-49 (1976).
- [13] Ya.G. Sinai, *Theory of Phase Transitions: Rigorous Results*. Oxford, New York: Pergamon Press (1982).
- [14] M. Zahradnik, *An Alternate Version of Pirogov-Sinai Theory*, *Comm. Math. Phys.*, **93**, 559 (1984).

- [15] J.Slawny, Low-temperature Properties of Classical Lattice Systems: Phase Transitions and Phase Diagrams, *Phase Transitions and Critical Phenomena*, C.Domb and J.L.Lebowitz, eds **11**, 128-205. London: Academic Press (1987).
- [16] E.Seiler, Gauge Theories as a Problem of Constructive Quantum Field Theory and Statistical Mechanics, *Lecture Notes in Physics*, **159**. Berlin, Heidelberg, New York: Springer (1982).
- [17] L. Šamaj, *J. Physique* **50**, 273 (1989).
- [18] J. K. Percus and L. Šamaj, *J. Stat. Phys.* **77**, 421 (1994).
- [19] F. di Liberto, G. Monroy and F. Peruggi, *Z. Phys. B* **66**, 379 (1987).
- [20] F. S. de Aguiar, L. B. Bernardes and S. G. Rosa, *J. Stat. Phys.* **64**, 673 (1991).
- [21] R. Baxter, *Exactly solved models in statistical mechanics*, Academic Press, London (1982).
- [22] *Finite Size Scaling and Numerical Simulation*, edited by V. Privman (World Scientific, Singapore, 1990); M.N. Barber, in *Phase Transitions and Critical Phenomena 8*, edited by C. Domb and J.L. Lebowitz (Academic, London, 1983).
- [23] K. Binder, *Z. Phys.* **B 43**, 119 (1981).
- [24] D.C. Radulescu and D.F. Styer, *J. Stat. Phys.* **49**, 281 (1987).
- [25] R. Dickman and G. Stell, preprint.

FIGURES

FIG. 1. Phase diagram in the M - z plane for a square lattice (MC) and for a Bethe lattice with coordination number $q = 4$. Lines: Exact results for the Bethe lattice for the transition lines from the gas phase to the crystal phase (dashed line), from the gas to the demixed phase (full line) and from the crystal to the demixed phase (dotted line). Symbols for MC: Transition points from the gas phase to the crystal phase (circles), from the gas to the demixed phase (triangles) and from the crystal to the demixed phase (squares).

FIG. 2. A schematic plot of the interplay among the disordered (dis), demixed 1 (d1) and demixed 2 (d2) Bethe solutions in the $[z, \rho(1)]$ plane for a) $M > 2$, b) $M = 2$; the solution with the lowest, intermediate and highest free energy is depicted by the solid, dashed and dotted line, respectively.

FIG. 3. Typical configurations for $M = 9$ and (a) $z = 0.1$, (b) $z = 5$ and (c) $z = 8.5$.

FIG. 4. Cumulant U_L versus z for $M = 9$. The different symbols refer to different subsystem sizes as indicated in the figure. Lines are for visual help.

FIG. 5. Cumulant U_L versus z for $M = 8$. The different symbols refer to different subsystem sizes as indicated in the figure. Lines are for visual help.

FIG. 6. Cumulant U_L versus z for $M = 7$. The different symbols refer to different subsystem sizes as indicated in the figure. Lines are for visual help.

FIG. 7. Phase diagram in the M - z plane for a square lattice (MC). Full lines: Asymptotic lines for the phase transitions in the high fugacity region, $M = z + 2 - 1/z$, and for the transition in the low fugacity region, $Mz = 3.7962$. Dashed lines: Results from the computation on the Bethe lattice with coordination number $q = 4$. Symbols for MC: Transition points from the gas phase to the crystal phase (circles), from the gas to the demixed phase (triangles) and from the crystal to the demixed phase (squares).

FIG. 8. (a) Cumulant U_L versus inverse system size for $M = 6$ and various values of z . (b) Cumulant U_L versus z for $M = 6$. The different symbols refer to different subsystem sizes as indicated in the figure. Lines are for visual help.

FIG. 9. Scaling functions of the order parameter (a) and the order parameter susceptibility (b) for $M = 20$ utilizing the 2D–Ising critical exponents. Lines indicate the asymptotic power law behavior with the 2D–Ising critical exponents ($t = |z - z_c|L^{1/\nu}$).

FIG. 10. Scaling functions of the order parameter (a) and the order parameter susceptibility (b) for $M = 15$ utilizing the 2D–Ising critical exponents. Lines indicate the asymptotic power law behavior with the 2D–Ising critical exponents ($t = |z - z_c|L^{1/\nu}$).

FIG. 11. Scaling functions of the order parameter (a) and the order parameter susceptibility (b) for $M = 10$ utilizing the 2D–Ising critical exponents. Lines indicate the asymptotic power law behavior with the 2D–Ising critical exponents ($t = |z - z_c|L^{1/\nu}$).

FIG. 12. Density of the system versus z for different number of components M , symbols refer to Monte Carlo results, the connecting lines are for visual help. The full (open) symbols refer to the MC results obtained by starting with configurations previously obtained for lower (higher) fugacities. The full line equals $\rho = z/(1 + z)$.

FIG. 13. Free energy $p_l(z)$ and $p_h(z)$ from thermodynamic integration for (a) $M = 15$ and (b) $M = 10$. The arrow at the z -axes indicates the transition value found by the phase stability study, see text.

FIG. 14. Scaling function of the order parameter for $M = 2$ (a), $M = 3$ (b) and $M = 4$ (c) using the 2D M -state Potts critical exponents. Lines indicate the asymptotic power law behavior with the 2D– M -state Potts critical exponents ($t = |z - z_c|L^{1/\nu}$).

FIG. 15. Scaling function of the order parameter susceptibility for $M = 2$ (a), $M = 3$ (b) and $M = 4$ (c) using the 2D M -state Potts critical exponents. Lines indicate the asymptotic power law behavior with the 2D- M -state Potts critical exponents ($t = |z - z_c|L^{1/\nu}$).

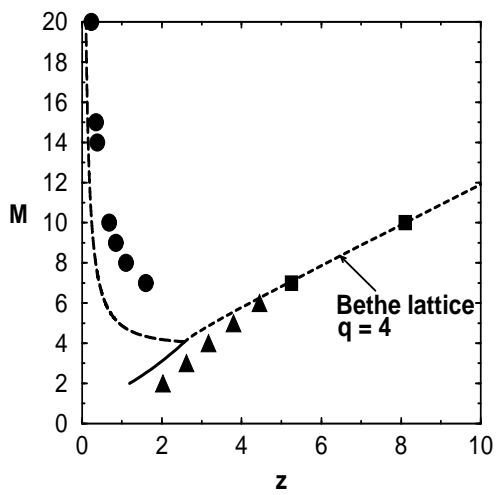


Figure 1:

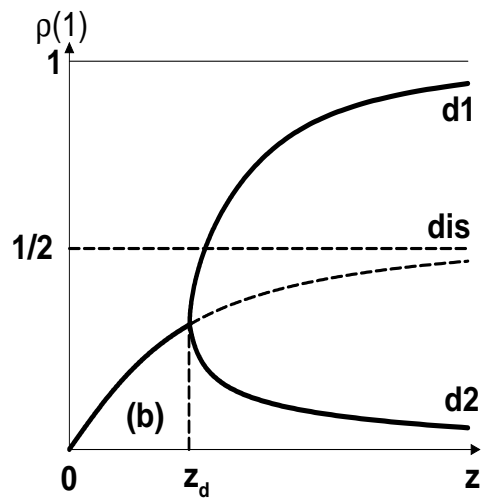
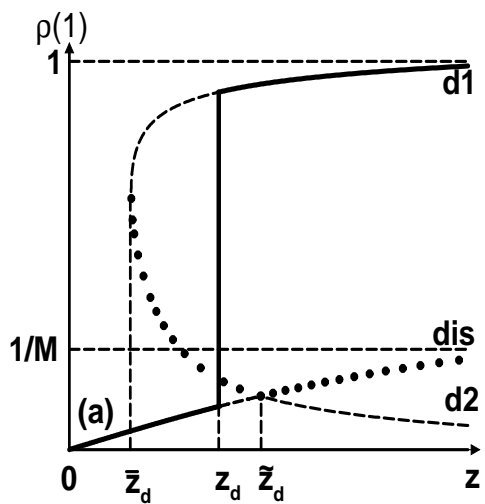


Figure 2:

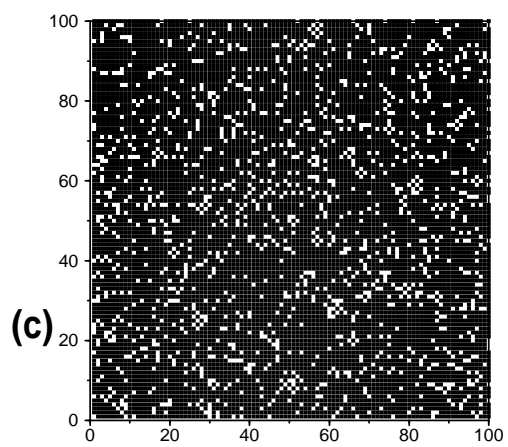
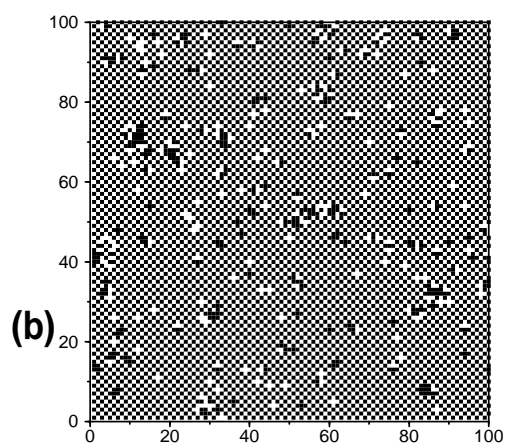
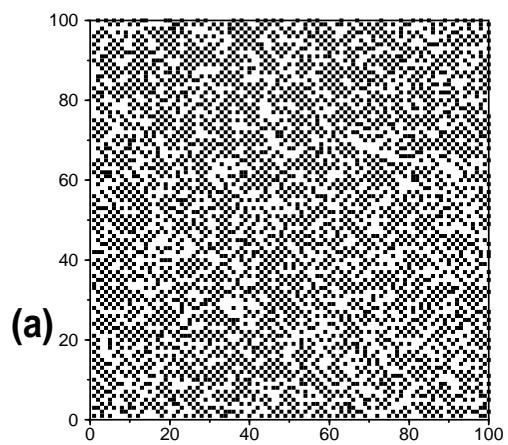


Figure 3:

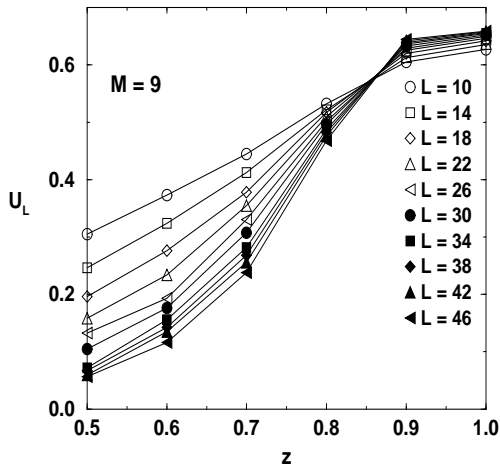


Figure 4:

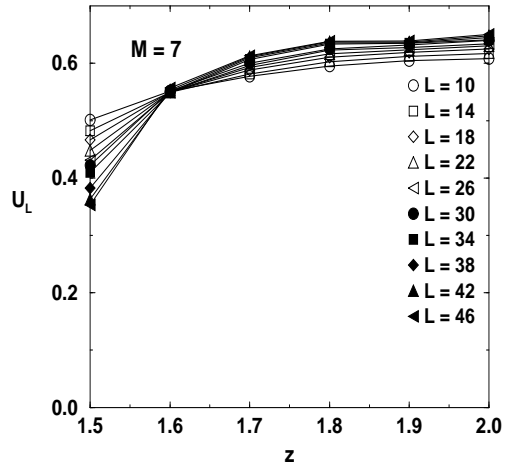


Figure 6:

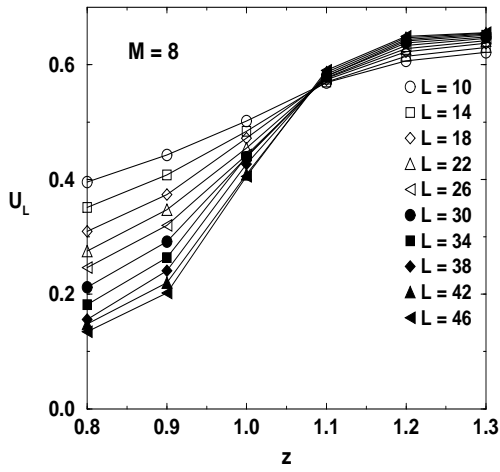


Figure 5:

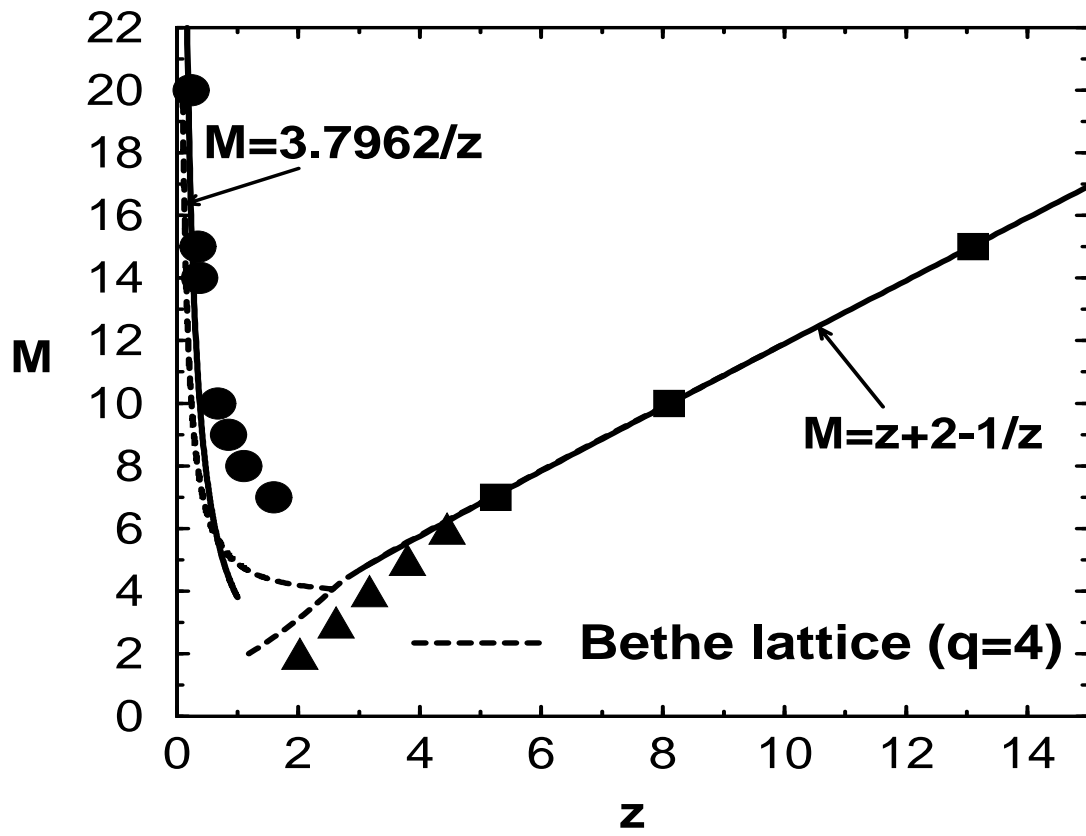


Figure 7:

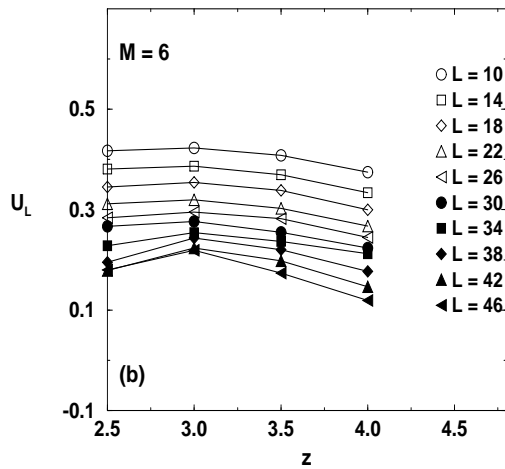
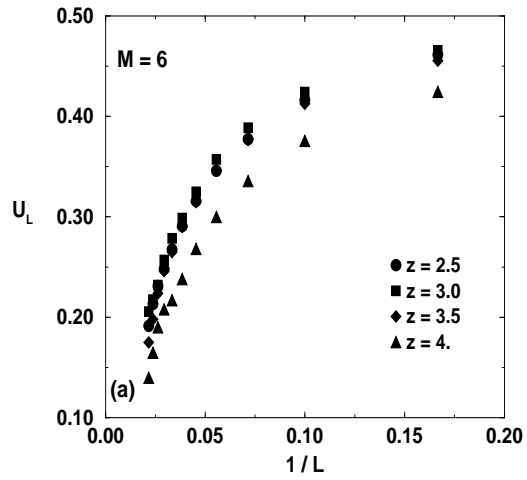


Figure 8:

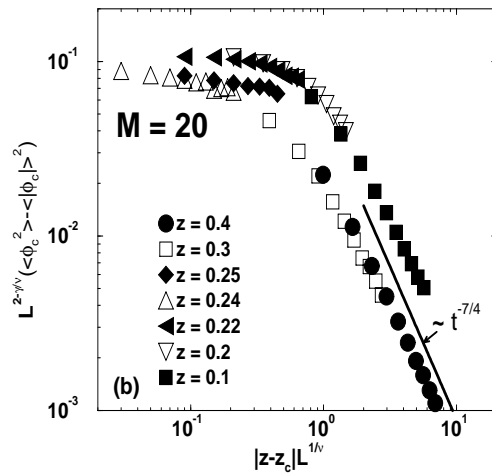
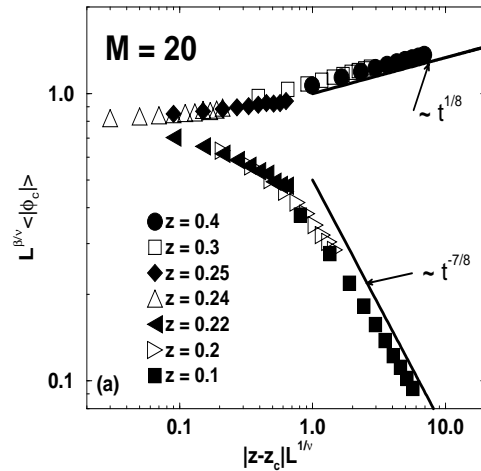


Figure 9:

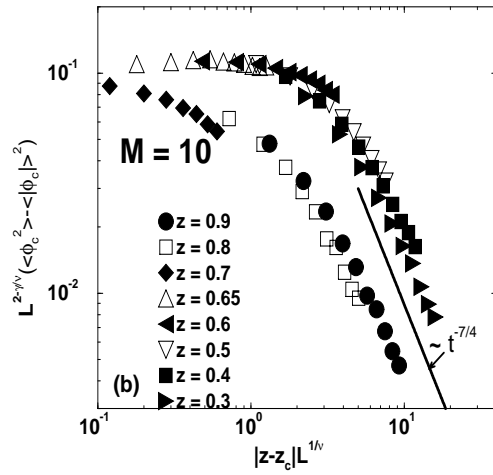
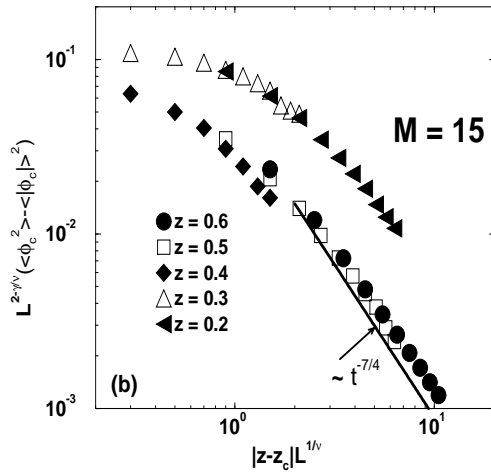
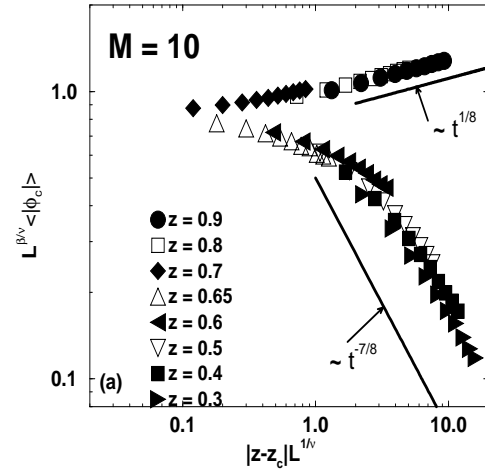
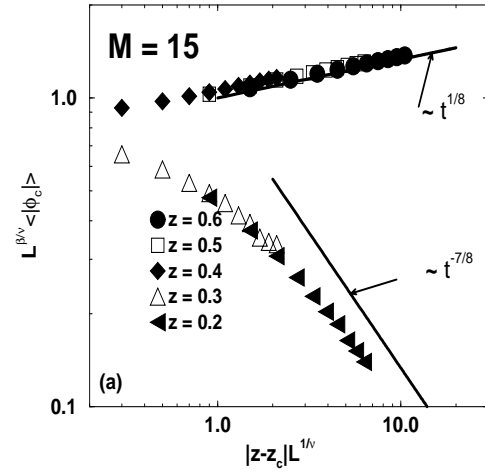


Figure 10:

Figure 11:

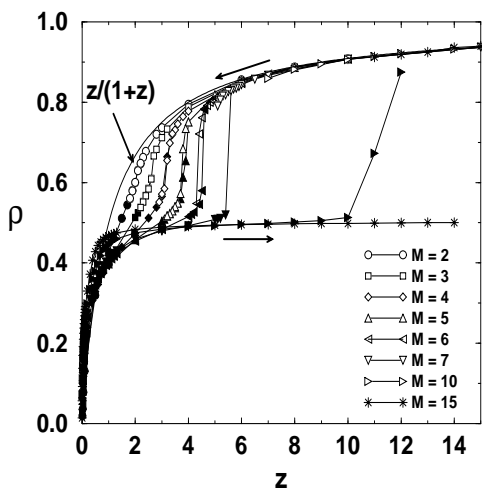


Figure 12:

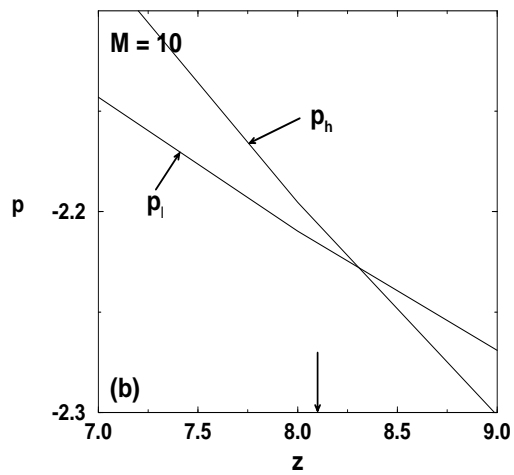
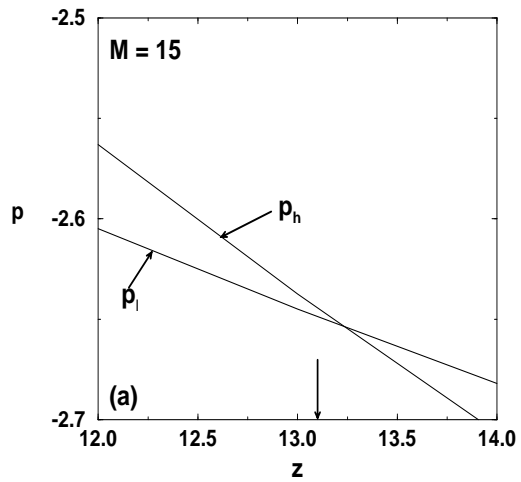


Figure 13:

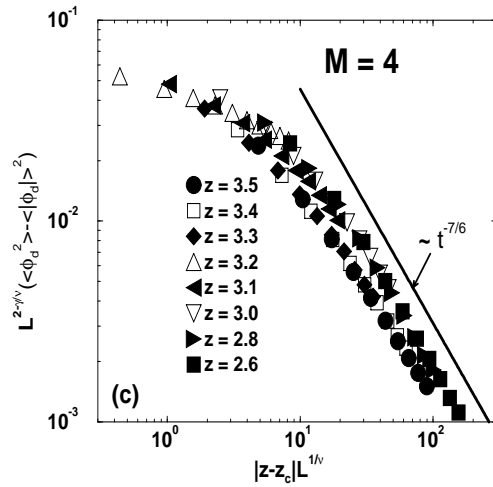
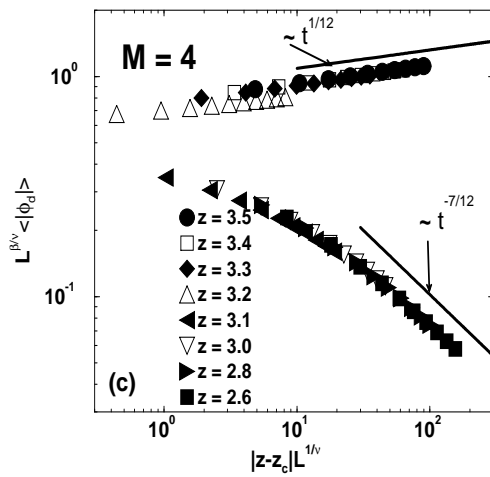
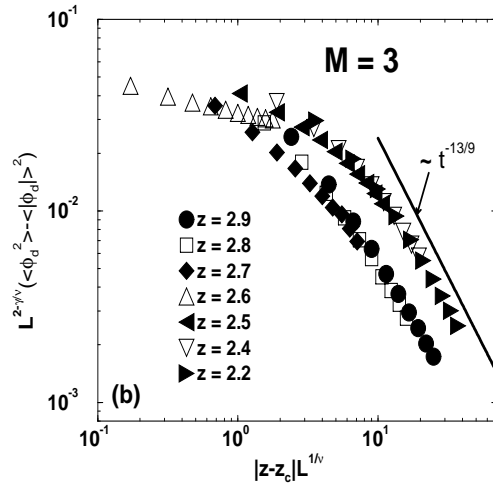
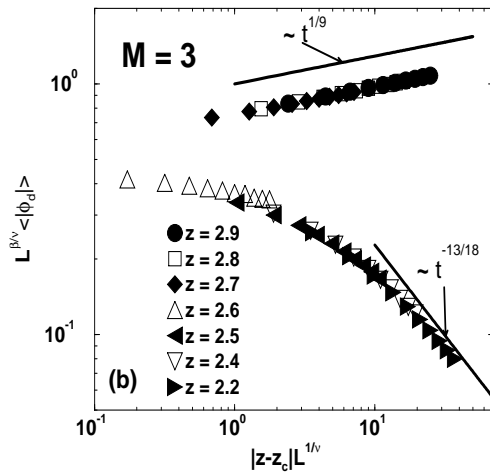
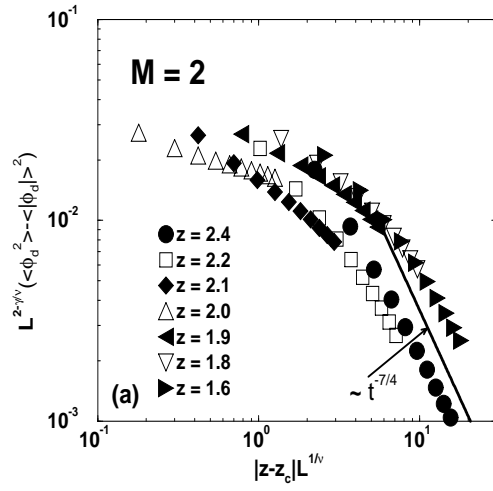
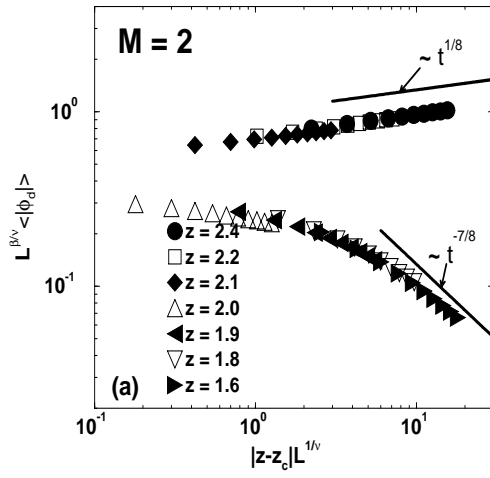


Figure 14:

Figure 15: